Cortical astrocytes rewire somatosensory cortical circuits for peripheral neuropathic pain

Sun Kwang Kim, Hideaki Hayashi, Tatsuya Ishikawa, Keisuke Shibata, Eiji Shigetomi, Youichi Shinozaki, Hiroyuki Inada, Seung Eon Roh, Sang Jeong Kim, Gihyun Lee, Hyunsu Bae, Andrew J. Moorhouse, Katsuhiko Mikoshiba, Yugo Fukazawa, Schuichi Koizumi & Junichi Nabekura

Supplemental data

Contents:

Legends for Supplemental Videos

Supplemental Video 1. Representative movie of astrocytic Ca^{2+} fluorescence in the S1 cortex of the control mouse. In vivo bolus dye loading (OGB-1 AM & SR101) and Ca^{2+} imaging of S1 astrocytes was performed using two-photon laser scanning microscopy (FV1000MPE, Olympus) and a Mai Tai DeepSee (Spectra Physics) mode-locked Ti:sapphire laser (power: under 10 mW) at an excitation wavelength of 800-850 nm. Time-lapse images of S1 (layer I) astrocytic Ca^{2+} fluorescence were recorded at 0.5 Hz for 10 min. Note that there are only infrequent Ca^{2+} transients across all the S1 astrocytes within the imaging frame in this control mouse.

Supplemental Video 2. Representative movie of astrocytic Ca^{2+} fluorescence in the S1 cortex of the PSL-early mouse. The imaging conditions and methods was the same as described for Supplementary Video 1. Partial sciatic nerve ligation (PSL) was performed 3 days prior to imaging, corresponding to the early phase of mechanical allodynia (PSL-early). Note the frequent Ca^{2+} transients across a large proportion of S1 astrocytes within the imaging frame in this PSL-early mouse.

Supplemental Video 3. Frequent neuronal Ca^{2+} transients in the IP_3R2-KO mouse following PSL injury. The imaging conditions and methods were the same as that described for Supplementary Videos 1 and 2, except that layer II/III neurons were imaged at 4 Hz for 3 min in IP_3R2-KO mice 3 days after PSL injury. Note the frequent neuronal Ca^{2+} transients, in contrast to few astrocyte Ca^{2+} transients in these PSL-early IP_3R2-KO mice (Supplemental Figure 1A).

Supplemental Figures

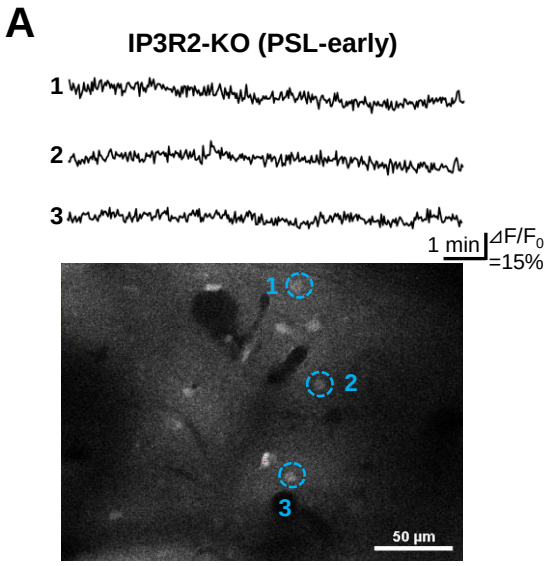

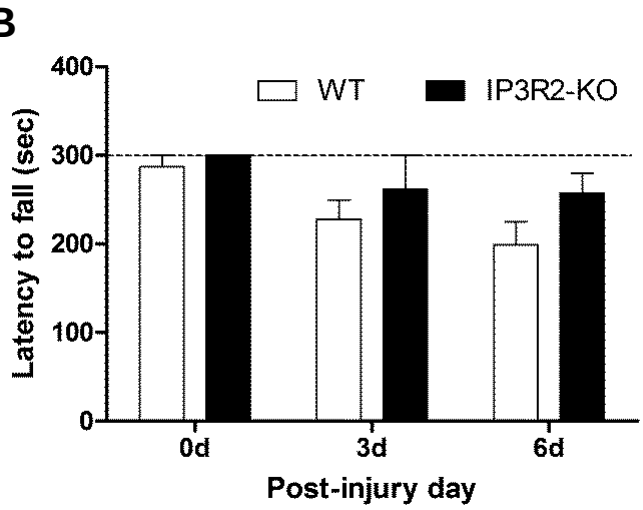

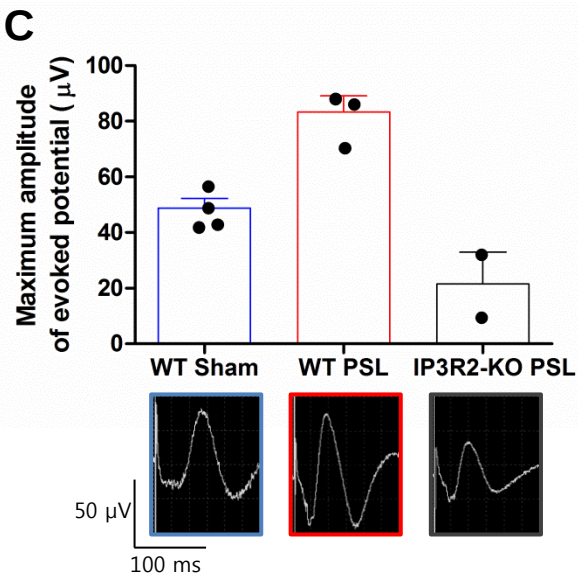

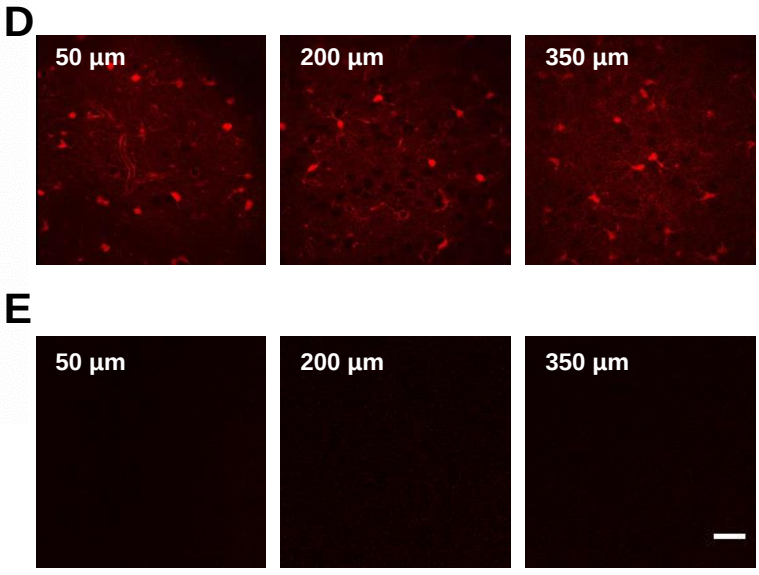

Supplemental Figure 1. Astrocytic Ca^{2+} transients and motor function in IP_3R2-KO mice, somatosensory-evoked potentials in S1 cortex following PSL injury, and specificity of Elvax-drug delivery. (A) In vivo two-photon Ca^{2+} imaging traces of S1 cortical astrocytes in IP_3R2-KO mice following PSL injury. Note that there observed no astrocytic Ca^{2+} transients. (**B**) The results for the rotatod test in WT (n=4) and IP_3R2-KO (n=3) mice before (0d) and after PSL injury. The mice were daily trained for the accelerating rotarod test (from 4 to 40 r.p.m. over 5 min) from 7 days before injury and the retention time (i.e. latency to fall) was recorded at 0d, 3d and 6d after injury. There was no significant difference between the two groups. (**C**) Somatosensory-evoked potentials in the S1 cortex of anesthetized mice. One week after PSL or sham injury, cortical field potentials evoked by electrical stimulation (10 V, 0.1 ms) of the right hind paw were recorded in the layer 1 of the left S1 cortex by using a tungsten electrode (5MΩ) as described previously [10]. (Top) Maximum amplitude of evoked potential in the WT PSL mice (n=3) was significantly bigger than that in the WT sham mice (n=4). Such enhanced evoked potential was not observed in IP_3R2-KO PSL mice (n=2). Error bars are mean ± SEM. (Bottom) Representative traces of somatosensory-evoked potentials for each group. (**D**) Selective staining of astrocytes by a topical application of SR101 into the S1 cortex using the Elvax drug delivery system. Three representative images were taken 50, 200 and 350 μm deep from the brain surface. A small piece of SR101 (100 μM)-soaked Elvax (2 mm × 2 mm) was placed on the dura matter over the S1 cortex through an open-skull cranial window. Three hours after the Elvax-SR101 implantation, low magnification image stacks of the S1 cortex (advancing from the surface to a depth of 600 μm, 0.41 μm/pixel) were collected using a two-photon microscope and an objective lens (60×, NA 0.9) at a two-photon laser excitation wavelength of 800 nm. (**E**) No staining of astrocytes in the S1 cortical region (50, 200 and 350 μm deep) about 1 mm apart from the implanted Elvax-SR101. Scale bar, 10 μm. These images were taken in the same condition as in (**D**), which contrastingly shows the clear staining of astrocytes in the cortical region just below the Elvax-SR101.

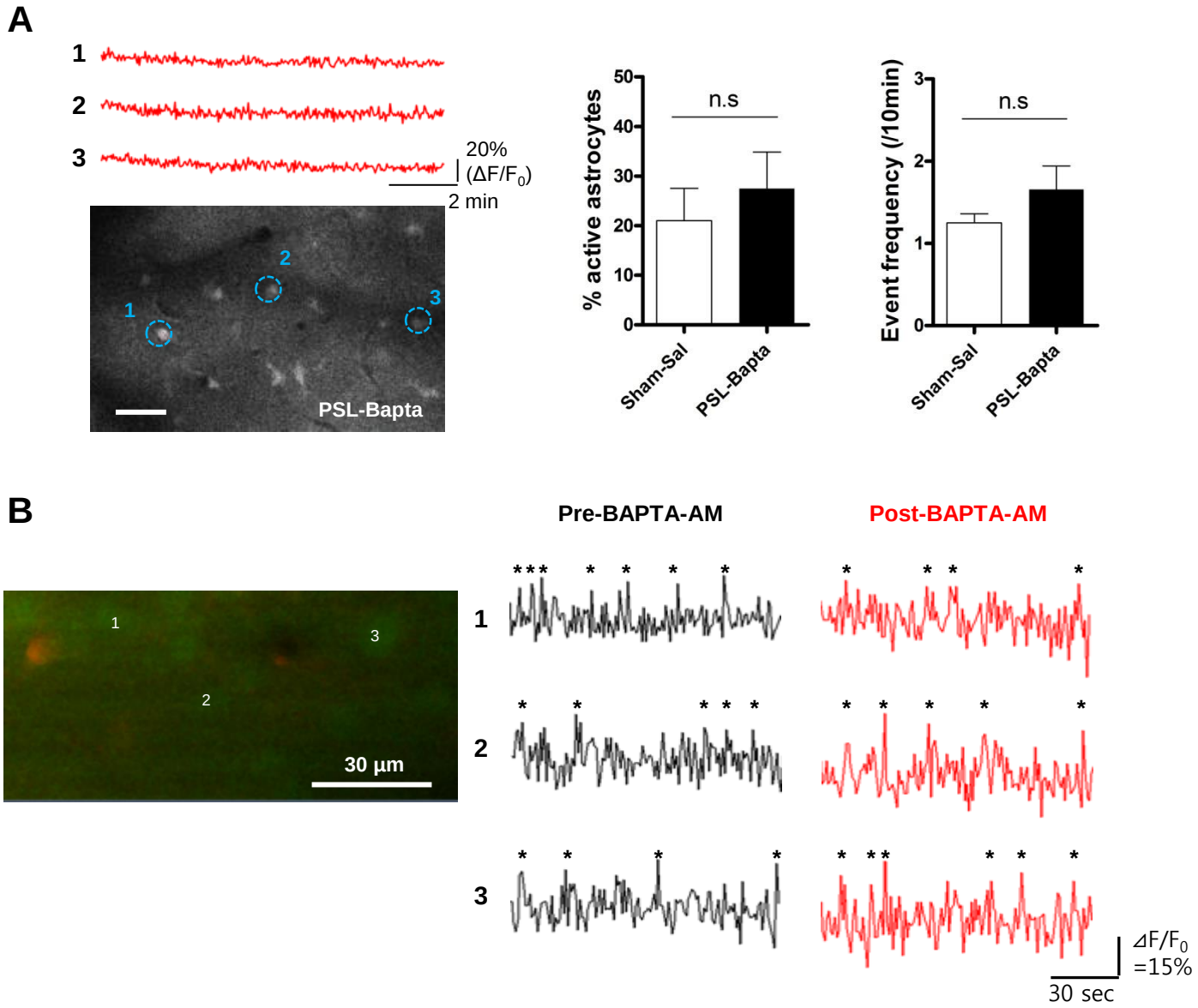

Supplemental Figure 2. **Pharmacological selective inhibition of S1 astrocytic Ca^{2+} transients in vivo.** (**A**) Left: Representative images of S1 astrocytes (bottom, dashed circles) and corresponding Ca^{2+} fluorescence traces (top) in PSL-BAPTA-AM mouse. Scale bar, 10 μm. Middle: Proportion of active astrocytes. N=9-10 imaged planes/group (n=3 mice/group). n.s.: *P*>0.05, Mann-Whitney test. Right: Corresponding mean Ca^{2+} event frequency of these active astrocytes. n.s.: *P*>0.05, Mann-Whitney test. Error bars are mean ± SEM. (**B**) In vivo two-photon Ca^{2+} imaging traces of S1 cortex layer II/III neurons (OGB-1 AM [green] positive, SR101 [red] negative) before and after BAPTA-AM infusion. Note that topical infusion of BAPTA-AM to the cortical surface in vivo did not affect neuronal Ca^{2+} activities. Asterisks indicate individual Ca^{2+} transients ($\Delta F/F_0$ > 15%).

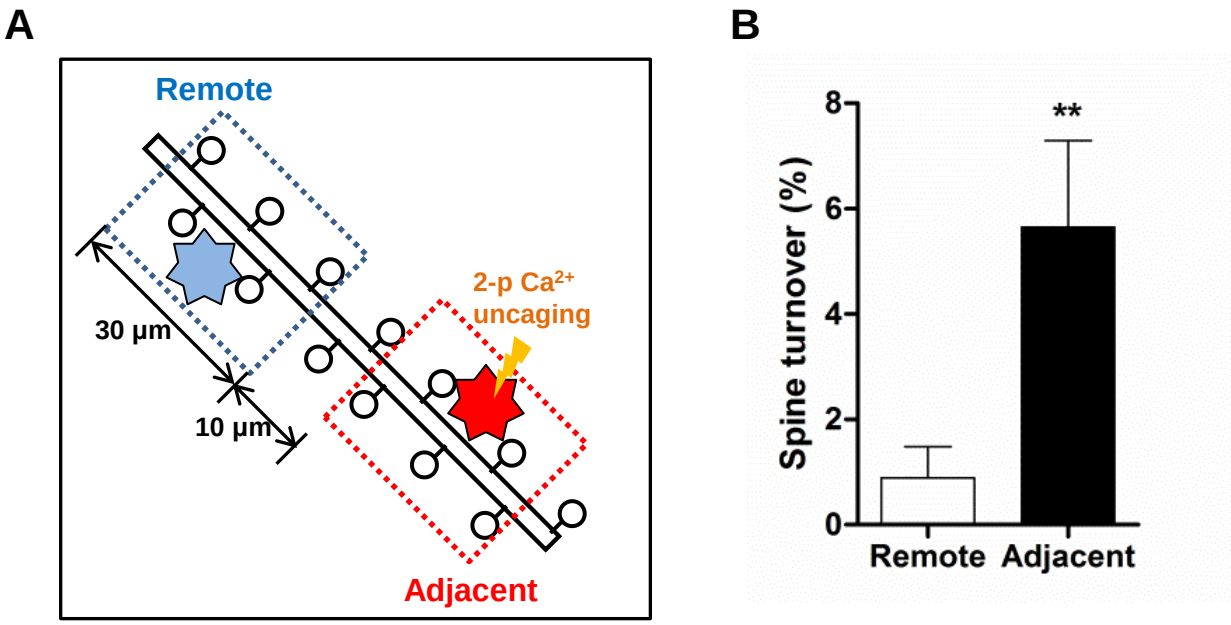

Supplemental Figure 3. **Spine turnover quantification for in vivo two-photon Ca^{2+} uncaging and repeated dendrite imaging.** (**A**) Schema for spine turnover quantification. Based on the published articles [Khakh & Sofroniew, 2015, *Nat Neurosci*] and our experience [see also Figure 2A] (single astrocyte occupies about 50 µm diameter and has well defined territory), "adjacent" dendritic segment was defined as 30 µm long dendritic segment with its 10 µm center located around the stimulated astrocyte. "Remote" dendritic segment is another 30 µm long dendritic segment that is at least 10 µm apart from the adjacent dendritic segment. (**B**) Quantitative analysis reveals that spine turnover rate in the adjacent dendritic segments is significantly increased as compared to remote dendritic segments (n=9 dendritic segments/5 mice). ***P*<0.01, Mann-Whitney test. .

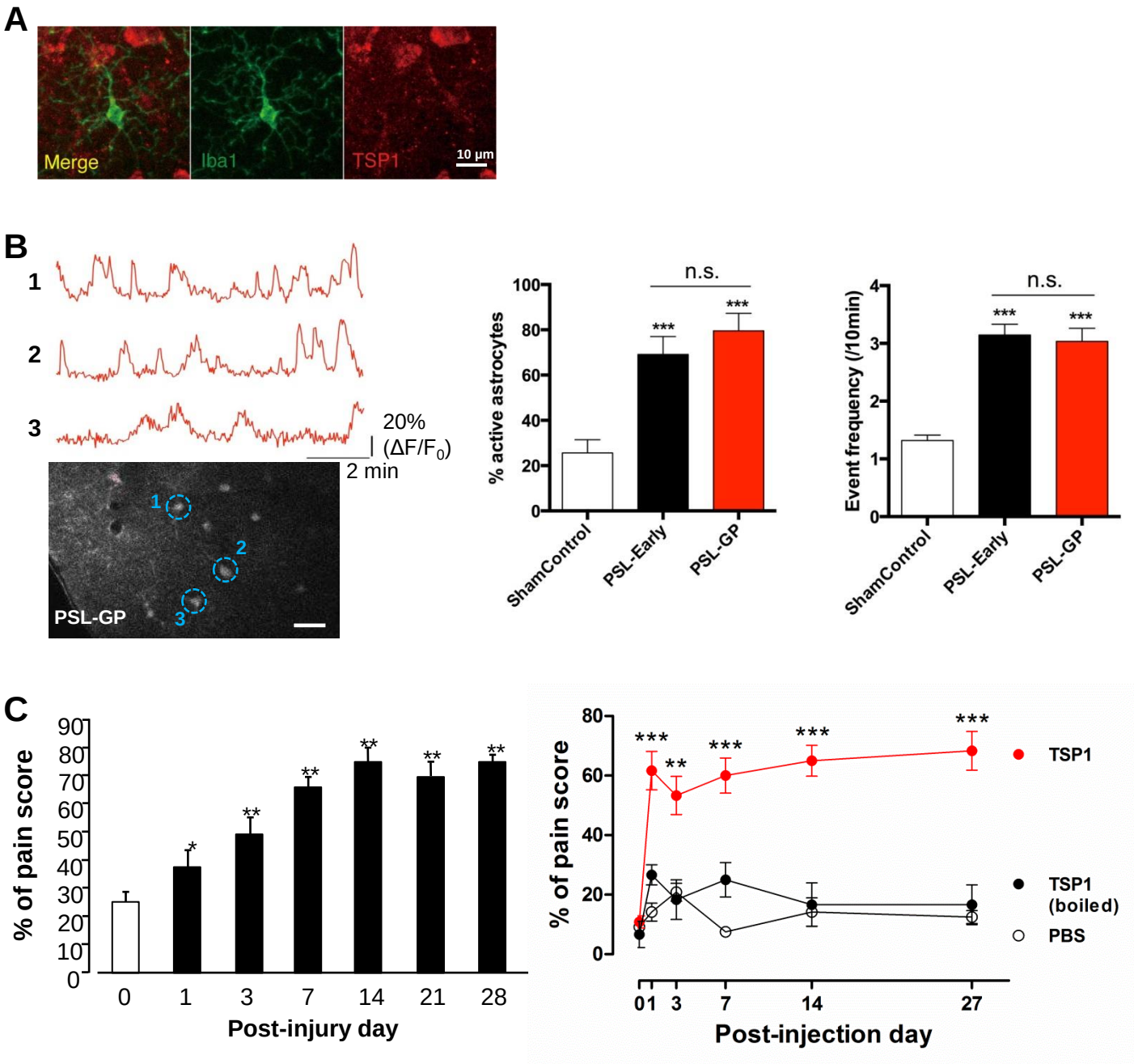

Supplemental Figure 4. **Immunohistochemistry for microglia and TSP-1, effect of gabapentin on S1 astrocytic Ca^{2+} transients, and the hind paw withdrawal response sensitivity following PSL injury or TSP-1 injection.** (**A**) Immunofluorescent image of S1 cortex from a PSL mouse showing a lack of co-localization of microglia (Iba-1, green) and TSP-1 (red). (**B**) Left: Representative images of three S1 astrocytes (bottom, dashed circles) in PSL-gabapentin (GP) mouse and their corresponding Ca^{2+} traces (Top). Right: GP did not affect the increase in S1 astrocytic Ca^{2+} transients seen after PSL injury. PSL-GP mice received a topical S1 infusion of gabapentin (5 mM) in the early phase of allodynia. Bar graphs show mean data of the proportion of active astrocytes (left graph; PSL-GP: n=8 imaged planes/3 mice) and S1 astrocytic Ca^{2+} event frequency (right graph; PSL-GP: n=89 cells/3 mice) in control, PSL and PSL-GP mice. Data for the ShamControl and PSL-Early groups are reproduced from Figure 1, C and D and shown for comparison. ***P<0.001, vs. ShamControl group, Kruskal-Wallis test. Note the lack of any significant difference (n.s.) in Ca^{2+} dynamics between PSL-Early and PSL-GP groups. The amplitude of Ca^{2+} events was not different amongst all three groups. (**C**) (Left) Time course of mechanical allodynia following PSL injury as measured using the hind paw withdrawal response sensitivity (% of maximum pain score). *P<0.05, **P<0.01, vs. pre-injury (0d) value (n=8 mice). Data from 0d to 21d post-injury are from our previous study [59]. Note that the time course of the early development of tactile allodynia (~7 days) and the later maintenance of allodynia was very similar to that shown in Figure 1C (measured with a mechanical threshold). (Right) Single injection of TSP-1 protein (n=6 mice), but not boiled TSP-1 (n=3) or PBS (n=6), into S1 cortex induced mechanical hypersensitivity lasting for at least 4 weeks. **P<0.01, ***P<0.001, one-way ANOVA. Error bars are mean ± SEM.

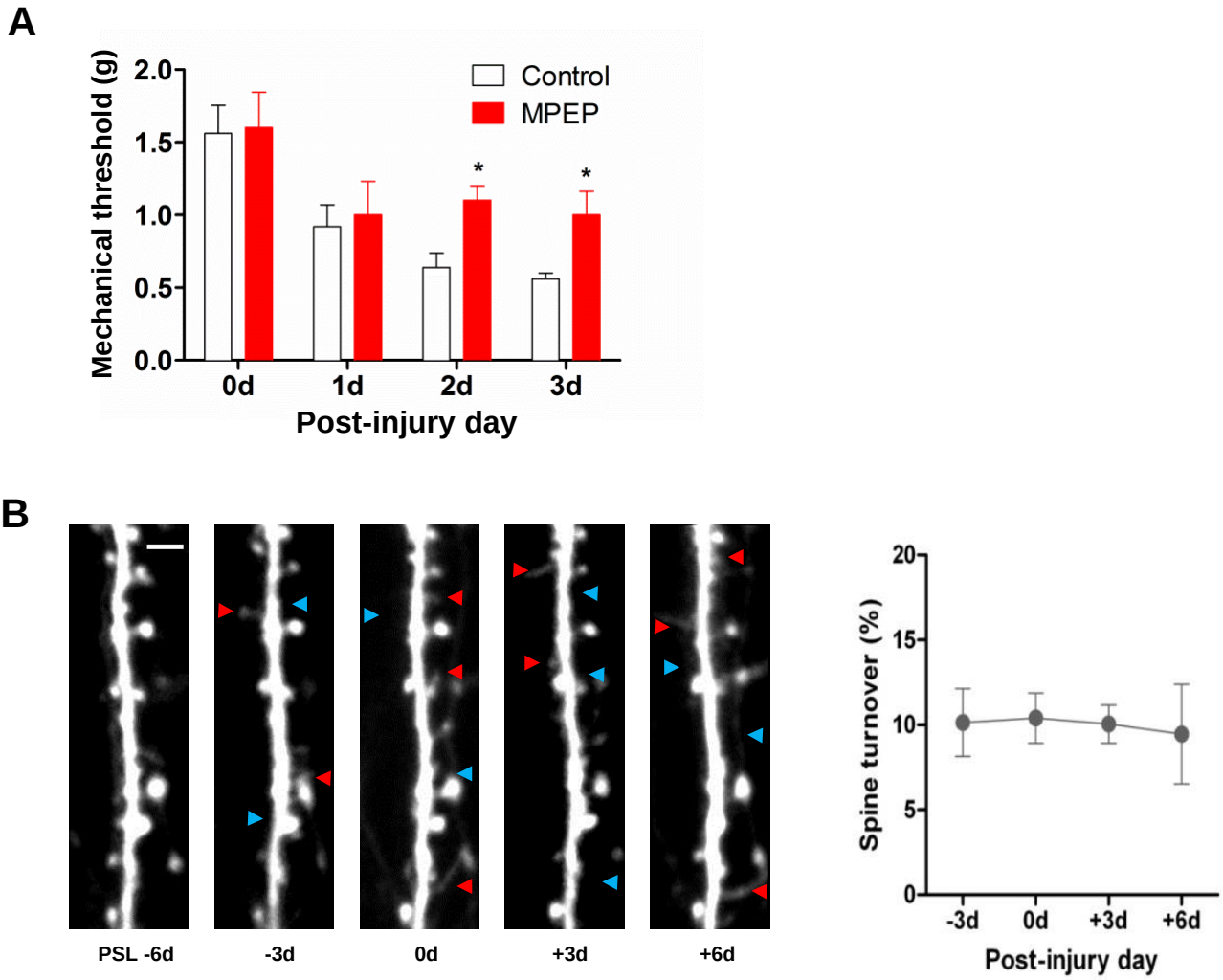

Supplemental Figure 5. **Short-term effect of mGluR5 blockade on mechanical allodynia and spine turnover in the barrel somatosensory cortex following PSL injury.** (**A**) Mean mechanical thresholds before (0d), and at 1d, 2d and 3d after PSL injury in MPEP- (n=4) or Saline-treated (n=5) mice. **P*<0.05, unpaired t-test. (**B**) Left: Representative images of the same dendrite in the barrel somatosensory cortex taken before and after nerve injury. Arrowheads indicate the spines generated (red) or eliminated (blue). Scale bar, 3 μm. Right: Spine turnover rate was not changed in the barrel somatosensory cortex following PSL injury. N=6 dendrites (total 145 spines) from 2 mice, *P*>0.05, one-way ANOVA. Error bars are mean ± SEM.

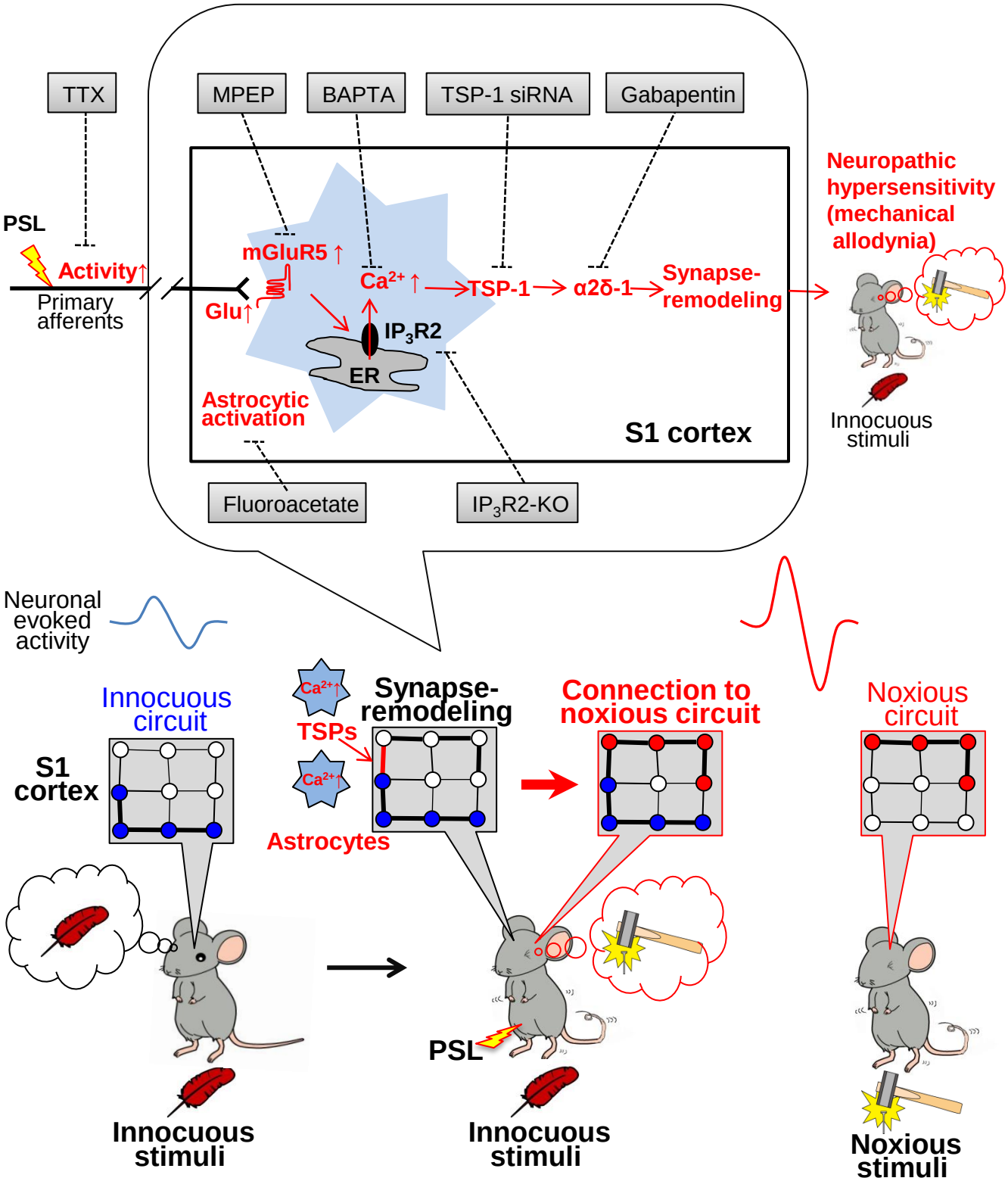

Supplemental Figure 6. **Schematic summary cartoon of reawakened cortical astrocytes-mediated synaptic rewiring in the S1 cortex for chronic neuropathic mechanical allodynia.** Peripheral nerve injury triggers a transient re-emergence of active immature-type astrocyte signaling within the S1 cortex during the first week post-injury time. Specifically, injury-induced afferent nerve hyperactivity [10,37,38] that increases extracellular glutamate levels in the S1 cortex to activate mGluR5s and mGluR-mediated elevation of astrocytic Ca^{2+} activity releases TSP-1 that binds to the neuronal $\alpha_2\delta$-1 receptors to initiate increased synapse remodeling. This probably increases the connections of the S1 innocuous circuits to noxious circuits, which might underlie the S1 circuit-level hyperexcitability to innocuous tactile stimuli as well as intracortical stimuli [9,10] and finally mediates the long-lasting mechanical allodynia.